American Journal of Quantum Chemistry and Molecular Spectroscopy
2025, Vol. 9, No. 1, pp. 1-11
https://doi.org/10.11648/j.ajqcms.20250901.11

Research Article

Synthesis and Characterisation of Cyclodextrin/ Sudan Black-B Caped ZnO/ Nanocrystals

Palanichamy Ramasamy[1], Ayyadurai Mani[2], Balakrishnan Sneha[1], Ezhil Nivetha[1], Albert Antony Muthu Prabhu[3], Govindaraj Venkatesh[4], Poomalai Senthilraja[5], Narayanasamy Rajendiran[1,*]

[1]Department of Chemistry, Annamalai University, Annamalai Nagar, India
[2]Center for Advanced Energy Materials, SRM TRP Engineering College, Tiruchy, India
[3]Department of Chemistry, Aditanar College of Arts and Science, Tiruchendur, India
[4]Department of Chemistry, Knowledge Institute of Technology (Autonomous), Salem, India
[5]Department of Bioinformatics, Bharathidasan University, Tiruchy, India

Abstract

Sudan black-B/cyclodextrin/zinc oxide (SBB/CD/ZnO) nanoparticles are prepared and characterized by various spectral and microscopic methods. Nanoparticle size was measured by TEM-EDS and X-RD methods. The effect of different polarities of the solvents, α-cyclodextrin (α-CD) and β-cyclodextrin (β-CD), on SBB was studied by various spectral methods. The inclusion behavior of SBB on both CDs was determined by the PM3 method. The doping effect of SBB/CD on ZnO nano was investigated by UV-visible, fluorescence, FTIR, DTA, XRD, FE-SEM, and TEM methods. The azo SBB dye has been included within the cyclodextrin cavities to form a noncovalent SBB/CD assembly in aqueous solution. The presence of an isosbestic point suggests that a 1:1 inclusion complex is formed. The HOMO-LUMO gap for the SBB/β-CD inclusion complex was more negative, which supports that this complex is more stable than SBB/α-CD inclusion complex. The SBB/CD capped ZnO nanocrystals absorb strongly in the visible region (425-650 nm) and emit at 520 nm. SBB absorption noted at 587 nm is moved to 650 nm in SBB/CD/ZnO, indicating efficient resonance energy transfer (RET) from the ZnO nano to the included SBB dye. FTIR, XRD, and TGA peaks of SBB/CD are different from ZnO/SBB/CD. SEM and TEM images showed nanocrystals are formed in ZnO/SBB/β-CD.

Keywords

Sudan Black-B, Zinc Oxide Nano, Cyclodextrin, Inclusion Complex, Nanocrystal

1. Introduction

Zinc oxide nanoparticles (ZnO-NPs) are a valuable and versatile metal oxide nanomaterial due to their unique physical and chemical characteristics, like- photocatalysts, sensors, and phosphors [1-5]. They possess high chemical stability, a

*Corresponding author: drrajendiran1967@gmail.com (Narayanasamy Rajendiran)

Received: 8 May 2025; **Accepted:** 22 May 2025; **Published:** 20 June 2025

broadened radiation absorption spectrum, a high electrochemical coupling coefficient, and high photostability with the molecular formula ZnO [6]. ZnO-NPs have been widely manufactured and utilized in various commercial and additive products, including ceramics, cement, plastics, glass, ointments, lubricants, adhesives, sealants, pigments, batteries, ferrites, fire retardants, cosmetics, and sunscreens, as well as in foods as a source of zinc nutrient [7, 8]. Generally, visible light-emitting ZnO nanocrystals would be ideal candidates as a replacement for cadmium-based fluorescent labels since they are nontoxic, less expensive, and chemically stable in air. However, nanoscale ZnO tends to aggregate or undergo aging because of high surface free energy, resulting in the disappearance of the visible emission. Attempts to stabilize the ZnO nanocrystals in solvent dispersions by capping have usually resulted in the quenching of the visible trap emission [7]. The visible emission involves deep trap states arising from oxygen vacancies and either electrons or holes in shallow trap states that originate from surface species/states in these large surface-to-bulk volume nanocrystals [8-12]. ZnO nanoparticles demonstrate significant antibacterial capabilities due to their small size, which can stimulate different bactericidal mechanisms once inside the bacterial cell, including the bacterial surface or bacterial core, generate ROS (reactive oxygen species), release Zn2+, and even be endocytosed by cells [7, 9, 10].

Here we describe a simple procedure to obtain ZnO nanocrystals that are stable over a range, and the water solubility is achieved by capping the ZnO nanocrystals with cyclodextrin (CD) cavities. Capping of nanocrystals by CD cavities is known to render the surface hydrophilic due to the existence of hydroxyl groups on the rim of the CD cavity [13-17]. A unique feature of the CD-capped ZnO nano crystals is that the surface-anchored CD cavities retain their host capabilities for the inclusion of small hydrophobic molecules. Here we show how the fluorescence properties of the water-soluble CD/ZnO nanocrystals can be modified by the hydrophobic organic dye, sudan black B, within the anchored cavities.

2. Experimental

2.1. Preparation of Drug/CD Inclusion Complex in Solution

Different concentrations of α-CD or β-CD solution (0.1 to 1.0×10-2 M) were taken in 10 ml standard measuring flask. SBB stock solution have a concentration of 2×10-2 M. SBB stock solution (0.2 ml) was added to the above flasks. The mixed solution was made up to 10 ml with triple-distilled water and shaken very well. The final SBB concentration in each flask was 4×10-4 M and 298 K temperature was used for the experiments.

2.2. Preparation of ZnO and SBB/CD/ ZnO Nanomaterials

0.01 M of zinc sulphate was dissolved in 100 ml of deionized water and the solution was heated to 50 - 60°C for 20 to 30 minutes. ZnSO4 and NaOH solution with a molar ratio of 1:2, which was carried out under vigorous stirring for 12 h at room temperature. The obtained white precipitate was washed several times and separated by centrifugation [13-19]. Finally, the precipitate (ZnO) was dried in an oven at 100°C for 6 h. The prepared ZnO nanoparticles showed a size distribution about 25-50 nm.

SBB (2×10-3 M) was dissolved in 20 ml of ethanol and gradually added to the CD (1×10-2 M in 80 ml) in deionized water. Then 0.01 M zinc sulphate (100 ml) was added to the above SBB/CD inclusion complex solution. Using a hot plate with a magnetic stirrer, this mixture was heated to 50°C for one hour. With vigorous stirring, one to two ml of 1% sodium hydroxide (1 g dissolved in 100 ml deionized water) was added and stirred for one to two hours. The above solution was frozen and dried (mini-lyophilized) at -80°C. The powder ZnO/SBB/CD sample was collected and used for further analysis.

2.3. Molecular Modeling Studies

Using the molecular modeling software Spartan 08, the molecular geometry of SBB, CD and its inclusion complexes were analyzed. The most stable complexation energy was determined theoretically after the structural assembly of two orientation inclusion complexes using the semi-empirical PM3 method in the gas phase and Gaussian 09W software.

3. Result and Discussion

3.1. Effect of Solvents, α-CD and β-CD

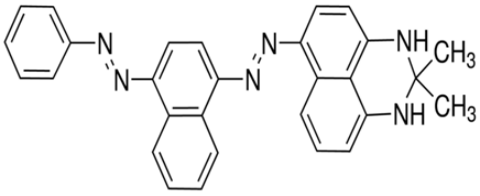

Figure 1. *Chemical structure of Sudan Black-B.*

Absorption and emission spectral maxima of sudan black-B (2,3-dihydro-2,2-dimethyl 4-[(4-phenylazo-1-naphthalenyl)-azo]-1H-perimidine, SBB, Figure 1) dye were measured in water, α-CD and β-CD (Table 1, Figure 2. In water, α-CD and β-CD, the absorption maxima of SBB were appearing at 587, 428, 290 nm, whereas a single emission maximum appeared at 427 nm. Upon increasing the

CD concentrations, no notable spectral changes were noticed in SBB, however, the absorbance and emission intensity rose at the same wavelength, indicating that the SBB molecule was entrapped into the CD cavities [20-35]. From the slope and intercept of the Benesi-Hildebrand plot, the binding constant for the inclusion complexes was estimated. The presence of an isosbestic point in the absorption spectrum and the plot of 1/(A-A0) vs 1/[CD] and 1/(I-I0) vs 1/[CD] confirms the formation of a 1:1 inclusion complex [20-35].

Table 1. *Absorption and fluorescence spectral maxima of SBB with different solvents and CD.*

Solvents	**λ_{abs}**	**log ε**	**λ_{flu}**
Cyclohexane	587	3.59	435
	413	3.35	
	286	3.50	
1,4-Dioxane	587	3.71	450
	414	3.45	
	288	3.60	
	240	3.88	
Ethyl acetate	592	3.68	450
	414	3.40	
	284	3.57	
	250	3.61	
Acetonitrile	589	3.79	450
	413	3.53	
	283	3.69	
	224	3.69	
2-Propanol	599	3.74	430
	415	3.46	
	283	3.65	
	236	3.82	
	213	3.88	
Ethanol	594	3.70	430
	423	3.48	
	284	3.64	
Water	587	3.81	427
	428	3.59	
	290	3.73	
α-CD (0.01 M)	587	4.08	427
	428	3.87	
	290	4.07	
β-CD (0.01 M)	588	4.07	427
	429	3.84	
	291	4.05	
α-CD K (1:1) $x10^5$ M^{-1}	79	-	238
β-CD K (1:1) $x10^5$ M^{-1}	111	-	227
α-CD ΔG ($kcalmol^{-1}$)	-10.9	-	-13.7
β-CD ΔG ($kcalmol^{-1}$)	-11.8	-	-13.6

Solvents	λ_{abs}	log ε	λ_{flu}
Excitation wavelength (nm)	-	-	350

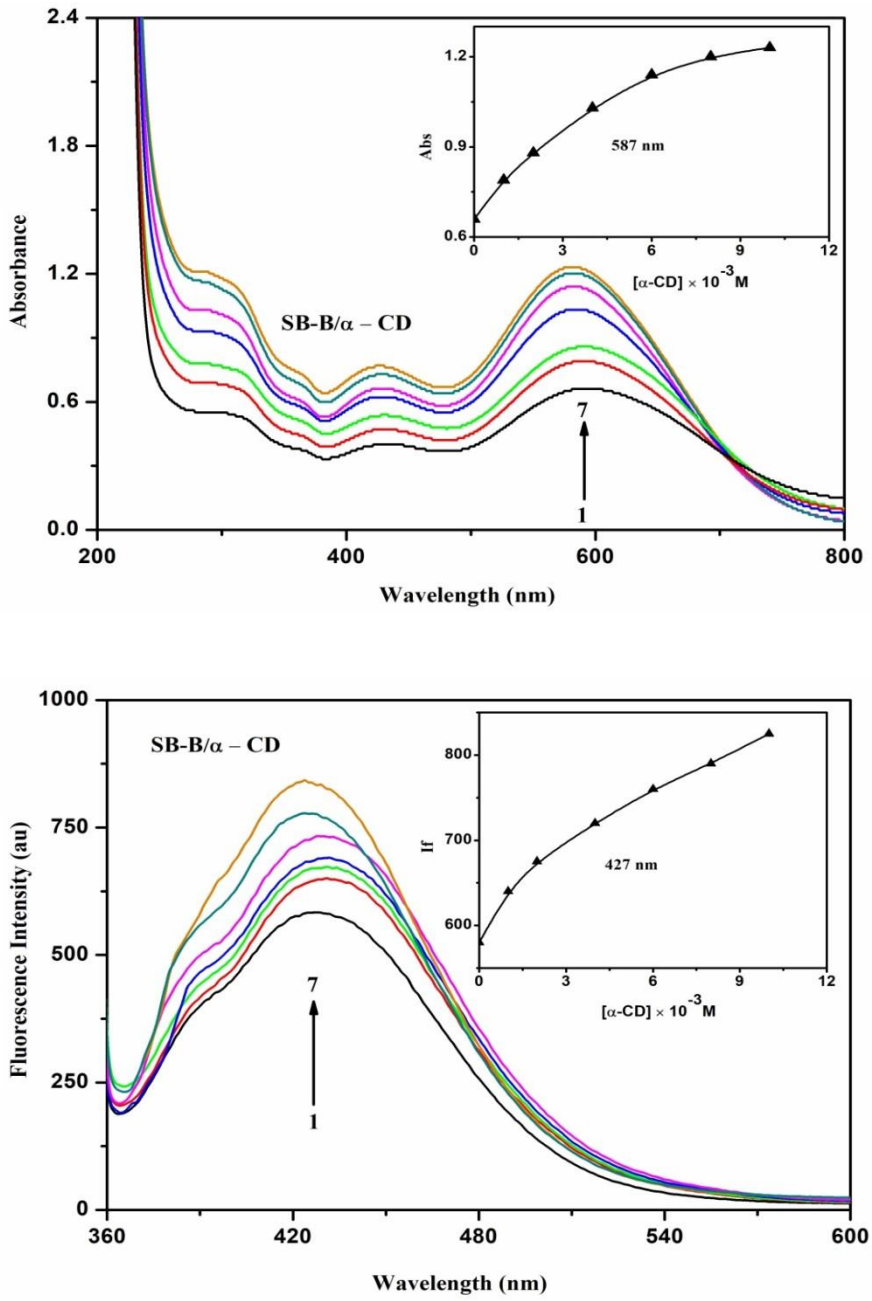

Figure 2. *Absorption and fluorescence spectra of SBB in different α-CD concentrations (M): (1) 0, (2) 0.001, (3) 0.002, (4) 0.004, (5) 0.006, (6) 0.008, (7) 0.01. Insert figure: absorbance/Fluorescence Intensity vs [α-CD].*

To know the inclusion complexation process, the absorption and emission spectra of the SBB molecule were examined in different solvent polarities (Table 1). Absorption maxima of the SBB molecule are red shifted from non-polar to aprotic solvents but blue shifted in water. In all the solvents, the SBB molecule exhibits a single emission. The absorption and emission spectral shifts are different in the solvents and the CD solution suggests the SBB molecule is encapsulated in the CD cavity. Because of the greater charge transfer effect of the NH and azo groups with the aromatic ring, a large red shift is observed in SBB. The red or blue shift in the absorption and emission spectral maximum reflects increased delocalization of the NH / azo groups and π-cloud of the conjugated double bonds [20-35].

3.2. Molecular Modeling

The ground state geometries of SBB, α-CD, β-CD and their inclusion complexes were optimized by PM3 method. HOMO, LUMO (Figure 3), binding energy, enthalpy, entropy, free energy, dipole moment, zero-point vibrational energy and Mullikan charge values for the SBB, α-CD, β-CD and the inclusion complexes are all listed in Table 2. When SBB entered the CD cavity, the polarity and the above parameter values for SBB, α-CD, β-CD significantly changed in the inclusion complexes [20-30].

Table 2. *Energetic features, thermodynamic parameters and HOMO-LUMO energy calculations for SBB and its inclusion complexes by semiempirical PM3 method.*

Properties	SBB	α-CD	β-CD	SBB/α-CD	SBB/β-CD
E_{HOMO} (eV)	-8.05	-10.37	-10.35	-8.15	-8.11
E_{LUMO} (eV)	-1.30	1.26	1.23	-1.42	-1.24
E_{HOMO} - E_{LUMO} (eV)	6.74	-11.63	-11.58	6.73	6.87
Dipole (D)	3.07	11.34	12.29	12.73	14.68
E (kcal mol^{-1})	-313.48	-1247.62	-1457.63	-1067.28	-1276.21
ΔE (kcal mol^{-1})	-	-	-	-133.14	-132.06
G (kcal mol^{-1})	-314.07	-676.37	-789.52	-998.08	-1023.75
ΔG (kcal mol^{-1})	-	-	-	-7.64	-79.84
H (kcal mol^{-1})	-253.55	-570.84	-667.55	-859.46	-1172.52
ΔH (kcal mol^{-1})	-	-	-	-35.07	-251.42
S (kcal/mol-Kelvin)	202.97	0.353	0.409	0.464	0.489
ΔS (kcal/mol-Kelvin)	-	-	-	-0.08	-0.12
ZPE	295.13	635.09	740.56	940.19	1234.55

kcal/mol; **kcal/mol-Kelvin; ZPE = Zero-point vibration energy

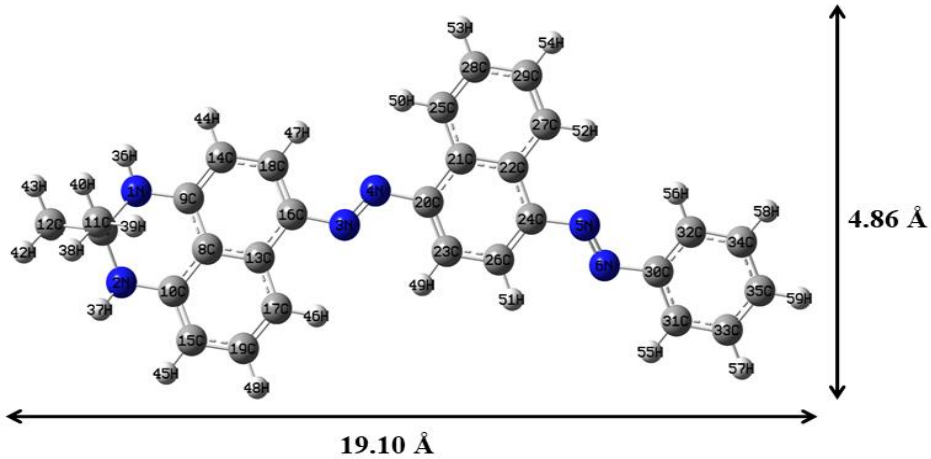

(a) Optimized structure

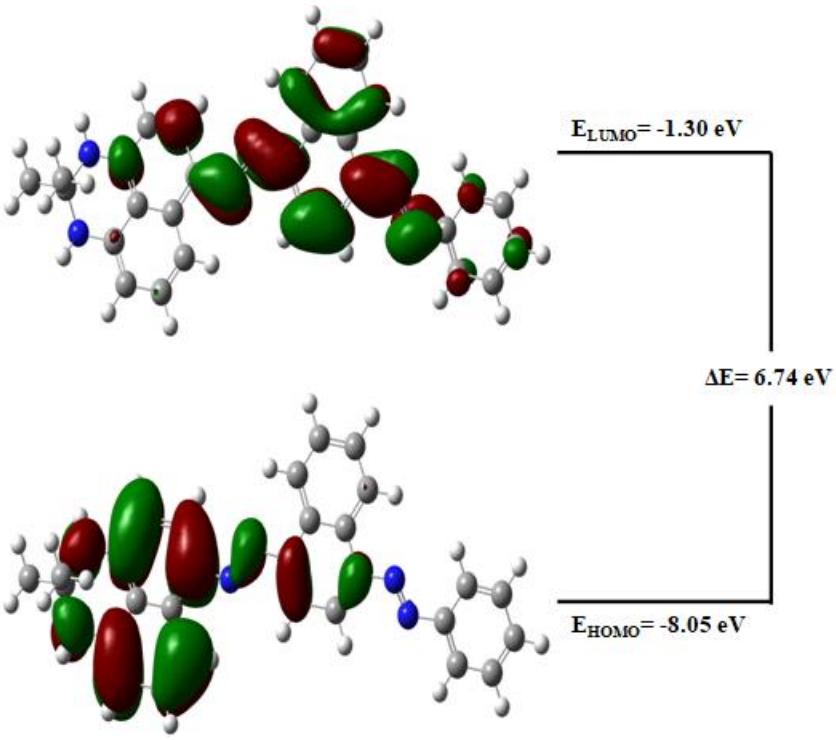

(b) HOMO, LUMO

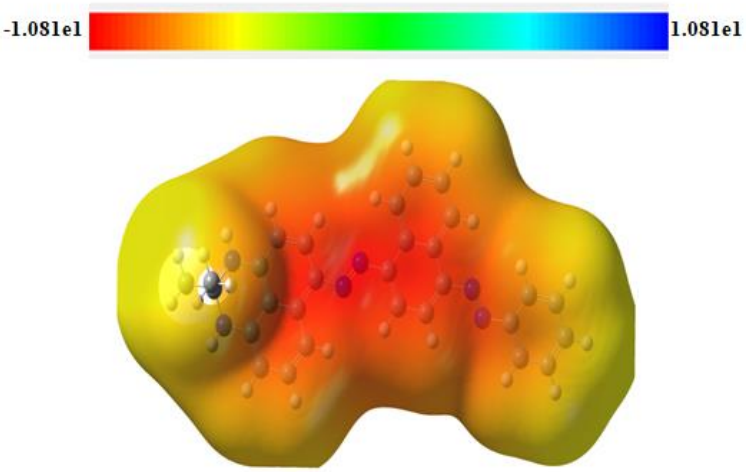

(c) MEP

Figure 3. *PM3 optimized structures of (a) SBB (b) HOMO, LUMO and (c) MEP of SBB. The blue color indicates for nitrogen atom, while in HOMO-LUMO, the green and red colors denote negative and positive phases of the molecules.*

The optimisation procedure was performed for two sets of coordinates, starting either with phenyl ring with azo group (Type I) and 2,3-dihydro-2,2-dimethyl group with naphthalene ring (Type II) of the SBB molecule encapsulated in the CD cavity (Figure 3). Compared to α-CD and β-CD, type I is more favorable than type II inclusion complex, because naphthalene ring with side chain size is larger than CD cavity. The internal diameter of the α-CD and β-CD is approximately 5.6 and 6.5 Å and the height is 7.8 Å, respectively. In SBB, the horizontal bond length is 19.10 Å and the vertical bond distance is 4.86 Å. The horizontal bond length of SBB is longer than the dimensions of the α-CD and β-CD cavities, hence, this molecule is partially encapsulated (i.e., either phenyl ring or 2,3-dihydro-2,2-dimethyl group with naphthalene ring of the SBB may encapsulate) in the CD cavity. The binding energy (ΔE), ΔG and ΔH values for the SBB/β-CD inclusion complex is more negative than SBB/α-CD complex. The negative Gibbs energy and enthalpy of the inclusion com-

plexes indicate that the formation of the complex is spontaneous and exothermic. The negative entropy (ΔS) effect suggests disorder of the system. The energy gap between HOMO and LUMO of the inclusion complexes suggest that there will be a significant change in the electronic structures and stability of the guest molecules while molecular recognition and binding. The red color in the molecular electrostatic potential's (MEP) figure (Figure 3) shows that the electronegative charge of the atoms is greater than that of other atoms.

3.3. Effect of SBB/CD Doping on ZnO Nanomaterials

The absorption and emission spectra of the ZnO, ZnO/SBB, ZnO/β-CD, ZnO/SBB/β-CD nanomaterials are examined. Absorption and emission bands of ZnO nanocrystals appear at 320 nm and 420, 355 nm, respectively [17-19]. It is known that ZnO nanoparticles exhibit their highest absorption in the 300-350 nm range. When SBB was doped to the ZnO nano, the above absorption and emission maxima altered to 600, 317 nm and 510 nm, respectively. With the addition of β-CD solution to the ZnO nano, the absorption and emission maxima shifted to 250 nm and 398 nm, respectively. When SBB/β-CD doped into the ZnO nano, the absorption and emission maxima shifted to 650, 425 nm and 525 nm, respectively. SBB absorption noted at 587 nm is moved to 650 nm in SBB/CD/ZnO, indicating efficient resonance energy transfer (RET) from the ZnO nano to the included SBB dye. Hence, the above red or blue shifts in the absorption and emission spectra suggest that SBB/CD doped on ZnO nano.

3.4. FE-SEM and TEM Images

ZnO nano, SBB, ZnO/β-CD and ZnO/SBB/β-CD nanomaterials were examined by FE-SEM and EDAX (Figure 4). ZnO particles form small size balls present in clusters, while ZnO/β-CD is appears in the sheet shape. SBB is present in a crystal shape, whereas ZnO/SBB/CD exists in a cloud shape image. FE-SEM-EDAX predicts the percentage of elements present in the nano: (a) ZnO nano contains 57.34% zinc and 42.66% oxygen, (b) ZnO/β-CD nano comprises 19.67% zinc, 54.42% oxygen and 25.91% carbon, (c) SBB dye contains 77.7% carbon, 22.30% nitrogen, and (d) The composition of ZnO/SBB/β-CD is 22.51% zinc, 27.01% carbon, 44.61% oxygen and 5.87% nitrogen. FE-SEM pictures and the atom composition of the nano ZnO, SBB are different from ZnO/SBB/β-CD confirms the formation of new nanocrystals.

TEM images of ZnO, ZnO/β-CD and ZnO/SBB/β-CD are displayed in Figure 5. Nano sheet like structures is found in the ZnO nanomaterials, while nanorod like structure is formed in ZnO/β-CD. ZnO nanosheet were seen to be uniformly spherical particles between 20 and 44 nm in size, while in ZnO/β-CD nano, the particle size was between 20 and 40 nm. ZnO/SBB/β-CD nanocrystal size was displayed to be between 18-26 nm. The formation of SBB/CD coated ZnO nanomaterial is supported by TEM-EDX data: (a) ZnO nano contains 69.84% zinc nano and 30.16% oxygen, (b) ZnO/β-CD nano comprises 8.79% zinc, 44.59% oxygen and 46.61% carbon, (c)) The composition of ZnO/SBB/β-CD is 74.97% zinc, 1.02% carbon, 3.81% oxygen and 20.18% nitrogen. The doping of SBB/β-CD on ZnO is confirmed by the EDX data.

The nanoparticles size is measured by X-RD and HR TEM methods. In XRD method, Scherer equation is used to measure the particle size: ZnO nano - 19.30 nm, β-CD - 23.84, SB-B- 25.56 nm, ZnO/β-CD - 20.69 nm, and ZnO/SBB/β-CD Nano - 17.34 nm. In HR-TEM, the nanocrystal size is measured by IMAGE-J software and the average particle size is calculated by Origin software: ZnO nano - 24.98 nm, ZnO/β-CD - 23.98 nm, ZnO/SB-B/β-CD Nano - 21.87 nm. Compared to XRD method, the 3-4 nm particle size is varied in HR-TEM method.

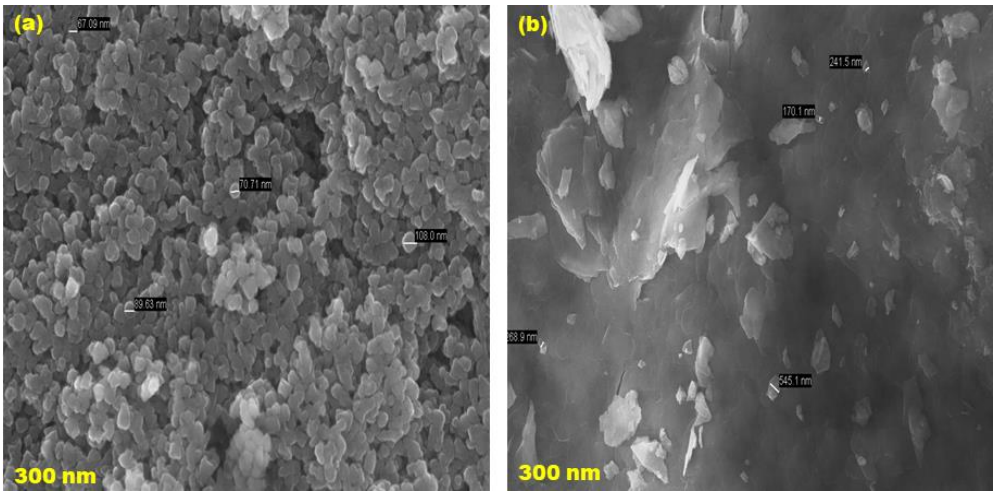

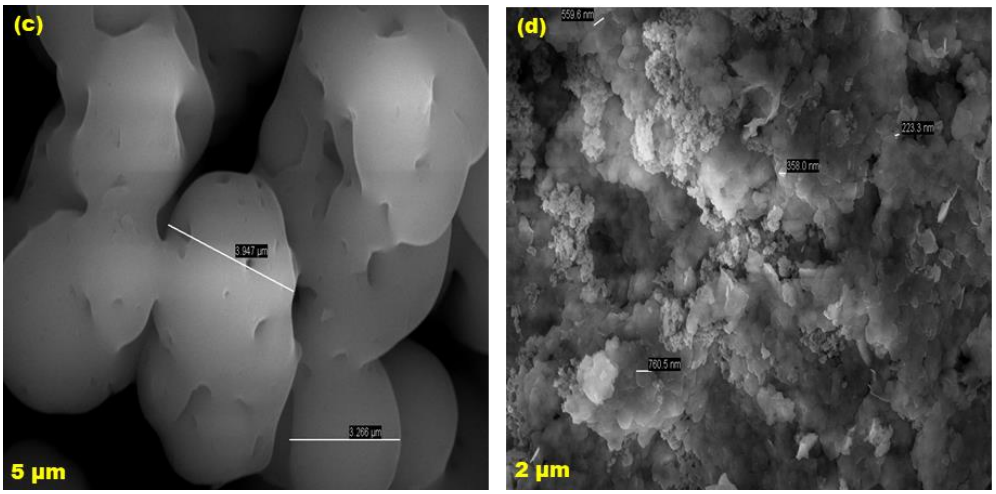

Figure 4. *FE-SEM images for (a) ZnO, (b) ZnO/β-CD, (c) SBB, (d) ZnO/SBB/β-CD inclusion complexes.*

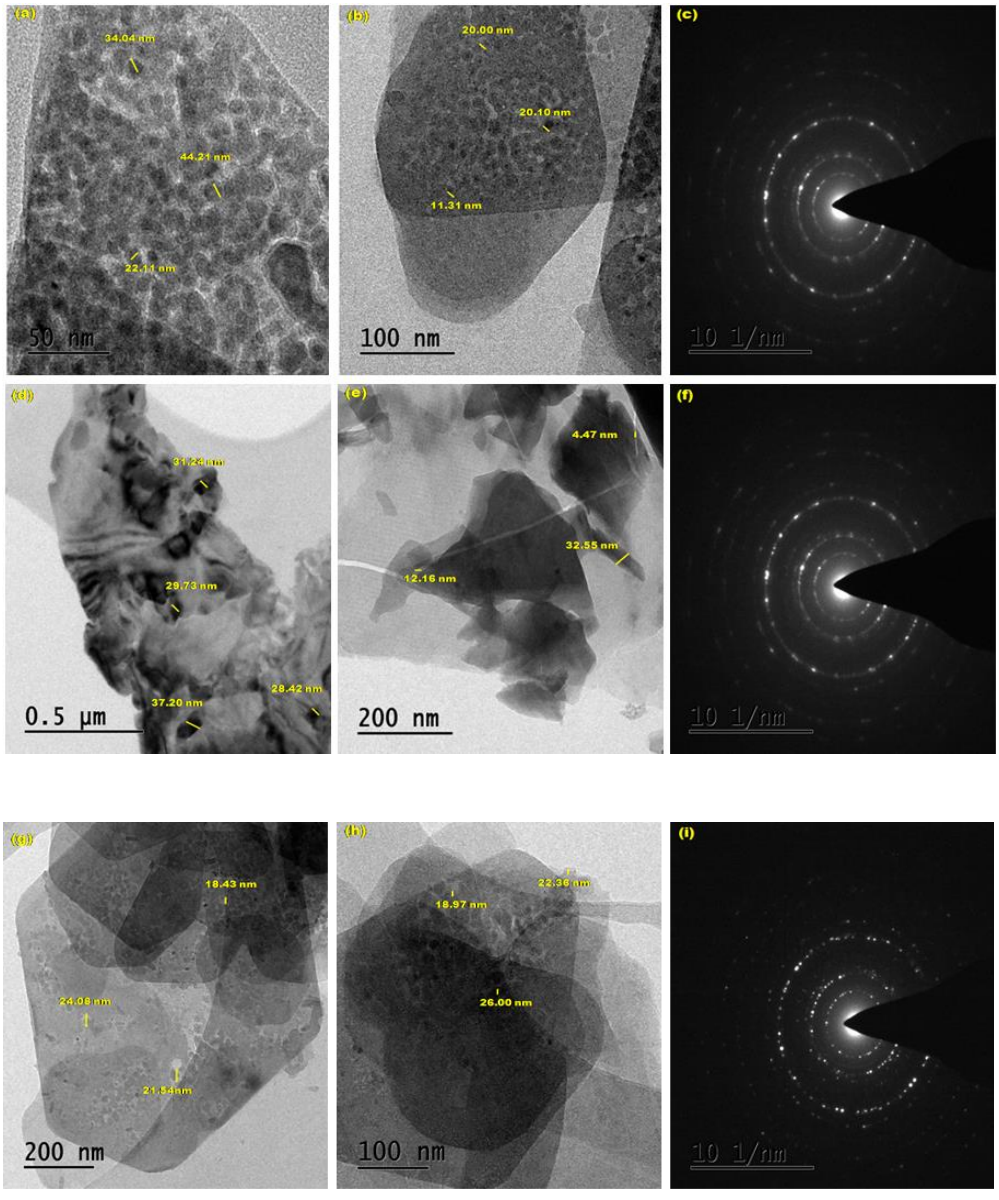

Figure 5. *TEM images for (a-c) ZnO, (d-f) ZnO/β-CD, (g-i) ZnO/SBB/β-CD.*

3.5. Powder X-ray Diffractogram

JCPDS: 03-065-3411 data and JCPDS card number 800-075 were used to determine the standard ZnO mineral name (3C, hexagonal closely packed, HCP) structure and the face-centered cubic peaks, respectively. The values of the hkl plane are found at (100), (002), (101), (102), (103), (110), (112) and (201) reflection planes of the hexagonal structure of ZnO. In ZnO, eight diffraction peaks are noted at 31.80, 34.51, 36.21, 47.52, 56.61, 62.90, 67.91, and 69.92. In β-CD, eight peaks were observed at 13.39, 19.93, 23.50, 27.65, 31.96, 35.54, 40.58, and 48.90, while in ZnO/β-CD ten peaks formed at 10.15, 15.18, 25.41, 28.38, 34.92, 42.29, 49.77, 59.16, 63.32, and 70.33. In SBB, three peaks formed at 15.70, 21.90, and 43.60, whereas in ZnO/SBB/β-CD twelve peaks formed at 8.30, 10.45, 16.39, 24.60, 28.65, 33.63, 36.73, 42.53, 50.70, 59.23, 64.35, and 69.88. Compared to isolated SBB, the XRD patterns of the ZnO/SBB/β-CD nanomaterials showed a different diffraction pattern and different peak intensities, suggesting that SBB/β-CD doped on ZnO nanomaterials.

3.6. Infrared Spectral Studies

FTIR spectra of ZnO nano, SBB, ZnO/SBB, ZnO/β-CD and ZnO/SBB/β-CD were measured. Due to the conversion of Zn+2 to ZnO nanoparticles, the FTIR frequencies of the ZnO nano were observed at 3325, 1587, 1450, 592 and 513 cm-1. The frequency appears at 3325 cm−1 indicating the presence of ZnO and the peaks at 592 and 513 cm-1 suggesting the presence of Zn nanoparticles. It is already reported, the FTIR spectrum of pure ZnO nanoparticles peak appearing at 595 cm−1 was the characteristic absorption of ZnO bond and the broad band peak at 3507 cm−1 can be attributed to the characteristic absorption of O-H group.

When β-CD was doped on the zinc oxide nano, the frequency at 3325 cm−1 shifted to 3280 cm−1, while the 1587, 1450 cm-1 frequencies moved to 1614, 1514 cm-1 and 592, 513 cm-1 peaks shifted to 594, 526 cm-1. The above variation in the FTIR frequencies indicates that the CD cavity covered the ZnO nanoparticles. In SBB, the azo group stretching frequency appears at 1541 cm-1, the naphthalene ring in plane bending frequency appears at 686, 530 cm-1 and the NH stretching frequency appears at 3330 cm-1. Aromatic ring stretching frequency appear at 1408 - 1619 cm-1, whereas out of plane peak appears at 939 cm-1 and C-NH stretching frequency appears at 1132 cm-1. C-CH3 stretching frequency appears at 2900 cm-1, while symmetric and anti-symmetric frequencies appear at 1359 and 1448 cm-1 respectively.

When SBB/β-CD doped on ZnO nano, the azo group stretching frequency was moved from 1541 cm-1 to 1512 cm-1, the naphthalene ring in plane bending frequency was shifted from 686, 530 cm-1 to 680, 592 cm-1 and NH stretching frequency was shifted from 3330 cm-1 to 3314 cm-1. Aromatic ring stretching frequency shifted from 1408 - 1619 cm-1 to 1450 - 1615 cm-1 whereas out of plane peak shifted from 939 cm-1 to 956 cm-1 and C-NH stretching frequency was moved from 1132 cm-1 to 1120 cm-1. CH3 stretching frequency appears at 900 cm-1 moved to 1016 cm-1, while symmetric and anti-symmetric frequencies appear at 1359 and 1448 cm-1 moved to 1367 and 1450 cm-1 respectively. Compared to SBB and ZnO/β-CD, ZnO/SBB/β-CD nanomaterials showed a marked change in the frequencies, suggesting that the SBB/CD was doped on ZnO nanocrystals.

3.7. DTA Thermogram

DTA profiles of pure ZnO nano, SBB, ZnO/β-CD and ZnO/SBB/β-CD are determined. In ZnO nano, two exothermic and three endothermic peaks were noticed at 226.1, 546.7°C and 272.6, 731.1, 919.2°C, respectively. SBB exhibits three exothermic peaks at 252.2, 513.1, 870.9°C and β-CD exhibits one exothermic peak at 128.6°C. In ZnO/β-CD, two exothermic and four endothermic peaks were noticed at 224.3, 932.4°C and 265.2, 354.6, 749.8, 884.1°C respectively. In SBB/β-CD/ZnO, two endothermic and two exothermic peaks appears at 285.6, 953.1°C and 720.4, 1003.5°C respectively. The endothermic peaks in the nanomaterials are caused by the loss of water from the CDs. In contrast to the pure SBB and ZnO a new peak arises in SBB/β-CD/ZnO, indicating the formation of the nanocrystals.

4. Conclusion

SBB/CD/ZnO nanocrystals are synthesized and characterized by UV-visible, fluorescence, FTIR, DSC, XRD, FE-SEM, and TEM methods. Single emission was observed in all the solvents, α-CD and β-CD. PM3 method shows, the horizontal bond length of SBB is longer than the dimensions of the α-CD and β-CD cavities, hence, this molecule is partially encapsulated in the CD cavity. SBB absorption noted at 587 nm is moved to 650 nm in SBB/CD/ZnO indicating efficient resonance energy transfer (RET) from the ZnO nano to the included the SBB dye. SEM and TEM images showed that nanocrystals are formed in ZnO/SBB/β-CD. Compared to XRD, the particle size of ZnO/SBB/β-CD in HR-TEM method is varied from 3-4 nm. Compared to isolated SBB, CD and inclusion complex, the XRD, TGA, and FTIR showed a different spectral behaviour confirm SBB/β-CD doped on ZnO nano.

Abbreviations

FTIR	Fourier Transform Infrared Spectroscopy
DTA	Differential Thermal Analysis
XRD	X-ray Diffraction
SEM	Scanning Electron Microscopy
TEM	Transmission Electron Microscopy

HOMO	Highest Occupied Molecular Orbital
LUMO	Lowest Unoccupied Molecular Orbital
SBB	Sudan Black B
ZnO NPs	Zinc Oxide Nanoparticles
A-CD	Alpha Cyclodextrin;
B-CD	Beta Cyclodextrin
PM3	Parametric Method 3
ΔE	Internal Energy Change
ΔH	Enthalpy Change
ΔG	Free Energy Change
ΔS	Entropy Change

Acknowledgments

This work was supported by the Rashtriya Uchchatar Shiksha Abhiyan (RUSA) Phase -2.0 [No. 128/A1/ RUSA 2.0, Health and Environment] New Delhi, India.

Author Contributions

The authors confirm contributions to the paper as follows:

Palanichamy Ramasamy: Experimental study

Ayyadurai Mani, Balakrishnan Sneha, Ezhil Nivetha, Poomalai Senthilraja: Calculation, Analysis, Data Collection

Albert Antony Muthu Prabhu, Govindaraj Venkatesh: PM3 calculation, Data interpretation

Narayanasamy Rajendiran: Manuscript draft preparation, Supervisor

Data Availability Statement

No data was used for the research described in the article.

Conflicts of Interest

The authors declare no conflicts of interest.

References

[1] Medintz, I. L., Uyeda, H. T., Goldman, E. R., Mattoussi, H. Quantum Dot Bioconjugates for Imaging, Labelling and Sensing. *Nat. Mater.* 2005; 4, 435-446. https://doi.org/10.1038/nmat1390

[2] Alivisatos, A. P. Semiconductor Clusters, Nanocrystals, and Quantum Dots. *Science*, 1996; 271, 933-937. https://doi.org/10.1126/science.271.5251.933

[3] Sabyasachi Rakshit, Sukumaran Vasudevan Resonance Energy Transfer from-Cyclodextrin-Capped ZnO: MgO Nanocrystals to Included Nile Red Guest Molecules in Aqueous Media, *ACS Nano,* 2008; 2, 1473-1479. https://doi.org/10.1021/nn800152a

[4] Dijken, A. V., Meulenkamp, E. A., Vanmaekelbergh, D., Meijerink, A. Identification of the Transition Responsible For the Visible Emission in ZnO Using Quantum Size Effects. *J. Lumin.* 2000; 90, 123-128. https://doi.org/10.1016/S0022-2313(99)00599-2

[5] Batista, P. D., Mulato, M. ZnO Extended-Gate Field-Effect Transistors as pH Sensors. *Appl. Phys.* Lett. 2005; 87, 143508-143510. https://doi.org/10.1063/1.2084319

[6] Wood, A., Giersig, M., Hilgendorff, M., Vilas-Campos, A., Liz Marzan, L. M., Mulvaney, P. Size Effects in ZnO: The Cluster to Quantum Dot Transition. *Aust J. Chem.* 2003; 56, 1051-1057. https://doi.org/10.1071/CH03120

[7] Norberg, N. S., Gamelin, D. R. Influence of Surface Modification on the Luminescence of Colloidal ZnO Nanocrystals. *J. Phys. Chem. B* 2005; 109, 20810-20816. https://doi.org/10.1021/jp0535285

[8] Bang, J., Yang, H., Holloway, P. H. Enhanced and Stable Green Emission of ZnO Nanoparticles by Surface Segregation of Mg. *Nanotechnology,* 2006; 17, 973-978. https://doi.org/10.1088/0957-4484/17/4/022

[9] Studenikin, S. A., Cocivera, M. Time-Resolved Luminescence and Photoconductivity of Polycrystalline ZnO Films. *J. Appl. Phys.* 2002; 91, 5060-5065. https://doi.org/10.1063/1.1461890

[10] Rakshit, S., Vasudevan, S. Trap-State Dynamics in Visible Light-Emitting ZnO: MgO Nanocrystals. *J. Phys. Chem. C* 2008; 112, 4531-4537. https://doi.org/10.1021/jp7109109

[11] Gerold, E., Antrekowitsch, H. A Sustainable Approach for the Recovery of Manganese from Spent Lithium-Ion Batteries via Photocatalytic Oxidation. *International Journal of Materials Science and Applications*. 2022; 11(3), 66-75. https://doi.org/10.11648/j.ijmsa.20221103.12

[12] Liu, J., Mendoza, S., Roman, E., Lynn, M. J., Xu, R., Kaifer, A. E., Cyclodextrin-Modified Gold Nanospheres. Host Guest Interactions at Work to Control Colloidal Properties. *J. Am. Chem. Soc. 1999;* 121, 4304-4305. https://doi.org/10.1021/la991519f

[13] Mani, A, Ramasamy, P, Antony Muthu Prabhu A, Rajendiran N, Investigation of Ag and Ag/Co bimetallic nanoparticles with naproxen-cyclodextrin inclusion complex. *J. Molecular Structure 2023;* 1284: 135301-10. https://doi.org/10.1016/j.molstruc.2023.135301

[14] Mani A, Venkatesh G, Senthilraja P, Rajendiran N, Synthesis and Characterisation of Ag-Co-Venlafaxine-Cyclodextrin Nanorods. *European J Advanced Chemistry Research, 2024;* 5: 9-16. https://doi.org/10.24018/ejchem.2024.5.1.147

[15] Mani A, Ramasamy P, Antony Muthu Prabhu A, Senthilraja P, Rajendiran N, Synthesis and Analysis of Ag/Olanzapine /Cyclodextrin and Ag/Co/Olanzapine /Cyclodextrin Inclusion Complex Nanorods. *Physics and Chemistry of Liquids, 2024;* 62: 196-209. https://doi.org/10.1080/00319104.2023.2297223

[16] Mani A, Ramasamy P, Antony Muthu Prabhu A, Senthilraja P, and Rajendiran N, Synthesis and Characterisation of Ag/Co/Chloroquine/Cyclodextrin Inclusion Complex Nanomaterials. *J Sol-Gel Science and Technology, 2025;* https://doi.org/10.1007/s10971-024-06620-5

[17] Ramasamy P, Mani A, Sneha B, Nivetha E, Venkatesan M, Rajendiran N, Azo-hydrazo tautomerism in Sudan Red-B and Cyclodextrin/Sudan Red-B doped ZnO nanomaterials. *J Molecular Structure, 2025;* 1329: 141423-32. https://doi.org/10.1016/j.molstruc.2025.141423

[18] Surabhi Siva Kumar, Putcha Venkateswarlu, Vanka Ranga Rao, Gollapalli Nageswara Rao, Synthesis, characterization and optical properties of zinc oxide nanoparticles, *International Nano Letters,* 2013; 3, 30. https://doi.org/10.1186/2228-5326-3-30

[19] Sukesh Kashiram Tumram, Rajdip Bandyopadhyaya, Zinc oxide nanostructures: Experiments probing their transformation to nanorods. *Materials Science and Engineering: B,* 2023; 296, 116569. https://doi.org/10.1016/j.mseb.2023.116569

[20] Venkatesh G. Saravanan J. Rajendiran N. Cyclodextrin covered organic micro rod and micro sheet derived from supramolecular self assembly of 2,4-dihydroxy azobenzene and 4-hydroxy azobenzene inclusion complexes. *Bulletin Chemical Society of Japan,* 2014; 87: 283-293. https://doi.org/10.1246/bcsj.20130255

[21] Rajendiran N. Sankaranarayanan R. K. Nanorod formation of cyclodextrin covered sudan dyes through supramolecular self assembly. *J. Experimental Nanoscience,* 2015; 10: 407-428, https://doi.org/10.1080/17458080.2013.840934

[22] Rajendiran N. Sankaranarayanan R. K. Azo dye/Cyclodextrin: New findings of identical nanorods through 2: 2 inclusion complexes. *Carbohydrate Polymers,* 2014; 106: 422-431. https://doi.org/10.1016/j.carbpol.2014.01.030

[23] Sankaranarayanan R. K. Venkatesh G. Jayashree Ethiraj, Pattabiraman M. Saravanakumar K. Arivazhagan G. Shanmugam R. Rajendiran N. Stepwise pesudopolyrotaxane nanostructure formation from supramolecular self-assembly by inclusion complexation of fast violet B with α- and β-cyclodextrins. *J. Molecular Structure,* 2022; 1262: 133080-89, https://doi.org/10.1016/j.molstruc.2022.133080

[24] Antony Muthu Prabhu A. Venkatesh G. Rajendiran N. Azo-Hydrazo tautomerism in 1-phenyazo-2-naphthol dyes in various solvents, pH and β-CD. *J. Fluorescence,* 2010; 20: 961-972. https://doi.org/10.1007/s10895-010-0642-0

[25] Venkatesh G. Antony Muthu Prabhu A. Rajendiran N. Azonium-Ammonium Tautomerism and Inclusion Complexation of 1-(2,4-diaminophenylazo) naphthalene and 4-Amino azobenzene. *J. Fluorescence,* 2011; 21: 1485-1497. https://doi.org/10.1007/s10895-011-0835-1

[26] Prema Kumari, J. Antony Muthu Prabhu, A. Venkatesh, G. Subramanian, V. K. Rajendiran, N. Effect of solvents and pH on β-CD Inclusion complexation of 2,4-dihydroxy azobenzene and 4-hydroxy azobenzene. *J. Solution Chem.,* 2011; 40, 327-347. https://doi.org/10.1007/s10953-010-9639-1

[27] N. Rajendiran, R. K. Sankaranarayanan, J. Saravanan, Nanochain and vesicles formed by inclusion complexation of 4, 4'-diamino benzanilide with Cyclodextrins. J. Experimental Nanoscience, 2015; 10: 880-899. https://doi.org/10.1080/17458080.2014.930523

[28] Prema Kumari, J. Antony Muthu Prabhu, A. Venkatesh, G. Subramanian, V. K. Rajendiran, N. Spectral characteristics of sulfadiazine, sulfisomidine: Effect of solvents, pH and β-CD. *Physics and Chemistry of Liquids,* 2011; 49, 108-132. https://doi.org/10.1080/00319104.2010.509724

[29] Siva, S. Thulasidhasan, J. Rajendiran, N. Host-guest inclusion complexes of propafenone hydrochloride with α- and β-cyclodextrins: Spectral and molecular modeling study. *Spectrochim Acta,* 2013; 115A, 559-567. https://doi.org/10.1016/j.saa.2013.06.079

[30] Venkatesh, G. Sankaranarayanan, R. K. Antony Muthu Prabhu, A. Rajendiran, N. Absorption and fluorescence spectral characteristics of norepinephrine, epinephrine, isoprenaline, methyldopa, terbutaline and orciprenaline drugs. *Physics and Chemistry of Liquids,* 2012; 50, 434-452. https://doi.org/10.1080/00319104.2011.597029

[31] Stalin, T. Vasantharani, P. Shanthi, B. Sekar, A. Rajendiran, N. Inclusion complex of 1,2,3-trihydroxybenzene with α- and β-cyclodextrins. *Indian J Chemistry*, 2006; 45A: 1113-1120.

[32] Sivakumar, K. Stalin, T. Rajendiran, N. Dual fluorescence of diphenyl carbazide and benzanilide: Effect of solvents and pH on electronic spectra. *Spectrochimica Acta,* 2005; 62A, 991-999. https://doi.org/10.1016/j.saa.2005.04.033

[33] Rajendiran, N. Balasubramanian, T. Dual fluorescence of syringaldazine. *Spectrochim Acta,* 2007; 68A: 894-904. https://doi.org/10.1016/j.saa.2007.01.004

[34] Antony Muthu Prabhu, A. Sankaranarayanan, R. K. Siva, S. Rajendiran, N. Intra molecular proton transfer effects on 2,6-diaminopyridine. *J. Fluorescence,* 2010; 20: 43-54, https://doi.org/10.1007/s10895-009-0520-9

[35] Rajendiran, N. Swaminathan, M. Spectral characteristics of 4-aminodiphenyl ether in different solvents and various pH. *J. Photochem. Photobiol. A: Chem.,* 1996; 93: 103-108. https://doi.org/10.1016/1010-6030(95)04189-3